Available online at www.sciencedirect.com

jmr&t Journal of Materials Research and Technology

journal homepage: www.elsevier.com/locate/jmrt

Optimal composition for radiation shielding in BTCu-x glass systems as determined by FLUKA simulation

M.A.M. Uosif [a,*], Shams A.M. Issa [b,c,***], Antoaneta Ene [d,1,**], V. Ivanov [f], A.M.A. Mostafa [a], Ali Atta [a], E.F. El Agammy [a], Hesham M.H. Zakaly [c,e,f,****]

[a] Physics Department, College of Science, Jouf University, P.O. Box: 2014, Sakaka, Saudi Arabia
[b] Department of Physics, Faculty of Science, University of Tabuk, Tabuk, Saudi Arabia
[c] Physics Department, Faculty of Science, Al-Azhar University, Assiut, 71452, Egypt
[d] INPOLDE Research Center, Department of Chemistry, Physics and Environment, Faculty of Sciences and Environment, Dunarea de Jos University of Galati, 47 Domneasca Street, 800008 Galati, Romania
[e] Istinye University, Faculty of Engineering and Natural Sciences, Computer Engineering Department, Istanbul, 34396, Turkey
[f] Institute of Physics and Technology, Ural Federal University, Yekaterinburg, Russia

ARTICLE INFO

Article history:
Received 16 March 2023
Accepted 12 June 2023
Available online 13 June 2023

Keywords:
Gamma shielding
TeO_2
FLUKA simulation
XCOM
Borate glass
RPE

ABSTRACT

In various medical, industrial, and nuclear facilities, it is very necessary to have enough shielding against the radiation released by regularly employed isotopes. In this work, we concentrate on nuclear security as well as the radiation shielding against gamma attenuation capabilities of the borate glasses, including Te and Cu. These glasses have the chemical form of (100-x)[$30B_2O_3$–$70TeO_2$]-xCuO, where x = 0, 0.005, 0.01, 0.015, 0.02 wt%. The systems were represented by five distinct samples, labelled as BTCu-20, BTCu-15, BTCu-10, BTCu-5, and BTCu-0, where the number refers to the percentage of CuO in the mixture and the remainder is made up of TeO_2 and B_2O_3. Through the use of FLUKA simulations, the basic characteristics associated with gamma shieldings, such as attenuation and transmission factors, were examined for the particular energy range of 238 –1408 MeV emitted from ^{133}Ba, ^{137}Cs, ^{60}Co, ^{152}Eu, and ^{232}Th. The effect of the systematic replacement of CuO by B_2O_3 and TeO_2 on the shielding qualities was explored in depth for gamma radiation. In addition, comparison research was carried out between the currently available borate glasses and the traditional shielding materials. According to the findings of the current investigation, the G_{HVL} was found to be its lowest at 238 keV with values of 0.87, 0.92, 0.98, 1.04, and 1.10 (cm) for BTCu-0, BTCu-5, BTCu-10, BTCu-15, and BTCu-20 glasses, respectively. This points to the possibility that the BTCu-0 sample might be used in radiation shielding applications, which would result in increased nuclear safety.

* Corresponding author. Physics Department, College of Science, Jouf University, P.O. Box: 2014, Sakaka, Saudi Arabia.
** Corresponding author. INPOLDE Research Center, Department of Chemistry, Physics and Environment, Faculty of Sciences and Environment, Dunarea de Jos University of Galati, Romania.
*** Corresponding author. Department of Physics, Faculty of Science, University of Tabuk, Tabuk, Saudi Arabia.
**** Corresponding author. Physics Department, Faculty of Science, Al-Azhar University, Assiut, 71452, Egypt.
E-mail addresses: Mauosif@ju.edu.sa (M.A.M. Uosif), shams_issa@yahoo.com (S.A.M. Issa), antoaneta.ene@ugal.ro (A. Ene), h.m.zakaly@gmail.com (H.M.H. Zakaly).
[1] The work of the author AE and APC was covered by "Dunarea de Jos" University of Galati, Romania.
https://doi.org/10.1016/j.jmrt.2023.06.107

1. Introduction

As the state of current technology continues to improve, an increasing number of applications are beginning to make use of radiation to broaden and simplify how the sector functions. Radiation is necessary for X-ray imaging and cancer treatment in the medical area. Radiation is also used in other industries, such as agriculture, to improve the quality of food production. The usefulness of radiation is only going to increase as more and more uses are discovered for it. On the other hand, in order to reap these advantages, one must always exercise extreme caution while working with radiation [1–3]. Ionizing radiation, which has enough energy to inflict long-term damage to living tissue, is one example of radiation that, if not properly dealt with, may be exceedingly damaging. Placing a substance between the source of the radiation and the human body is one of the most popular and effective ways to shield humans from the harmful effects of radiation. Radiation shields are the name given to these types of materials, and over the last few decades, a significant amount of research has been carried out to make radiation shields as effective as possible for the purposes for which they were designed [4–12]. Depending on the kind of radiation that has to be shielded, the energy level of the radiation, the object that needs to be protected, and any other external considerations that need to be taken into consideration, radiation shields may take on a wide variety of shapes and sizes [13,14].

There are several varieties of glass, each distinct according to the characteristics of the glass forming. B_2O_3 is one of the most widely used glass formers because borate glasses have a diverse range of uses, including radiation shielding and optical glasses. B_2O_3 is one of the most widely used glass formers [15,16]. B_2O_3 glasses are highly sought after due to the fact that they have a low melting point, a high level of transparency, a cheap cost, a high level of thermal stability, an easy production process, and a high level of solubility. In addition, incorporating various glass modifiers and intermediates cause the coordination number of boron to rise from three to four. This results in an increase in the connectedness and stiffness of the glass system, which produces structurally more robust glass. As various oxides are incorporated into the glass, not only may the composition of the glass itself change, but so can some of its other qualities.

In order to be used successfully and efficiently in the application of interest, the vast majority of radiation technologies call on a diverse set of material qualities. Historically, silica glasses were considered a viable option due to their availability, ease of manufacturing, resistance to corrosion, thermal and mechanical stability, and optical clarity [17]. As the technology for radiation shielding continues to advance, new aspects of the material, including optical transparency, increased stiffness, and high density, have been the focal areas of focus for researchers [18]. TeO_2 is a fantastic option that is superior to P_2O_5, SiO_2, and other glass-forming oxides in this respect [19–22]. Because of its remarkable properties, tellurite glasses are increasingly used in optical technologies [23]. To increase the effectiveness of other glass-forming and modifying oxides in terms of their optical, physical, shielding, and mechanical characteristics, TeO_2 is often combined with other oxides. When used in glass compositions specifically incorporating TeO_2, B_2O_3 has outstanding glass-forming ability, optical transparency, thermal stability, hardness, and rare earth solubility. Compared to the other oxides, it has the highest hardness [24]. The copper present in glasses may be found in the form of free copper atoms, Cu^{2+} ions, or cu^{+} ions [25]. Since CuO plays a modifiable function in glass systems, it is able to enhance the physical, optical, and other qualities of glasses, which may then be taken into account in a variety of different technological applications [26,27].

Glasses containing heavy metal oxides have been developed recently as an alternative shield material with good features brought about by their transparency, lightweight, portability, good radiation absorbing ability, and ease of fabrication in various techniques. This was done to overcome the disadvantages of opaque and conventional materials [28]. Since this, a study on a novel system based on borotellurite glass that has been doped with copper oxide has been initiated since no researchers have yet conducted an inquiry into the radiation-shielding qualities of this material. This investigation has used a mixture of copper oxide and tellurium oxide to assess the usefulness of the aforementioned elements in the aforementioned applications. This research aimed to examine the radiation shielding capacity of TeO_2–B_2O_3–CuO glasses at different energies to better understand the radiation shielding ability of many additions of CuO.

2. Materials and methods

For the purpose of this study, five glass specimens from a series were chosen because they exhibited the weight-percentage formula TeO_2–B_2O_3–CuO. (Table 1). Umar [27]

Table 1 – Elemental compositions and density of all glasses.

Sample Code	Weight fraction (wt%)			ρ (g/cm^3)
	TeO_2	B_2O_3	CuO	
BTCu-0	0.700	0.300	0.000	4.370
BTCu-5	0.697	0.299	0.005	4.100
BTCu-10	0.693	0.297	0.010	3.710
BTCu-15	0.690	0.296	0.015	3.640
BTCu-20	0.686	0.294	0.020	3.500

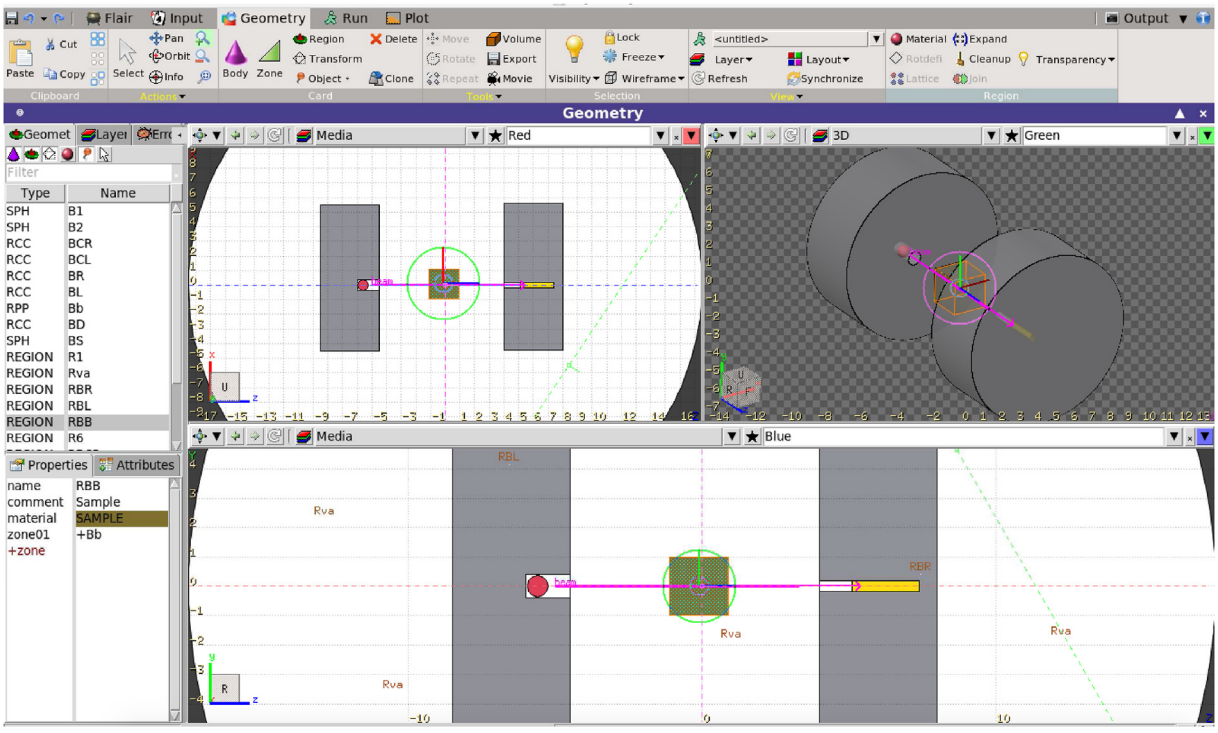

Fig. 1 – Utilizing FLUKA Monte carlo simulation to calculate attenuation parameters.

has recently synthesized the specified glasses, and they have documented the structural and optical characteristics of these samples. Employing the FLUKA modelling [29–33], we intended to investigate these glasses' radiation shielding properties during this study (Fig. 1). The linear attenuation coefficient, often known as the G_{LAC}, is the fundamental radiation shielding parameter. This coefficient is determined for every material by the Lambert-Beer law, which is as follows:

$$I = I_o e^{-G_{LAC}x}$$

We can obtain the mass attenuation coefficient (G_{MAC}) for any given medium by using the G_{LAC}, which is then stated using the mixing rule:

$$G_{MAC} = \sum_i W_i \left(\frac{G_{LAC}}{\rho}\right)_i$$

The relative difference (Δ, %) between G_{MAC} results obtained using the FLUKA code and those obtained via XCOM has been calculated using the following formula:

It is possible to provide both the half-value layer (G_{HVL}) and the mean free path (G_{MFP}) [34]:

$$G_{HVL} = \frac{Ln\,(2)}{G_{LAC}}$$

$$G_{MFP} = \frac{1}{G_{LAC}}$$

3. Results and discussion

Within the framework of the narrow beam geometry technique, the measuring procedure makes use of gamma rays originating from ^{232}Th (238 and 911 keV), ^{152}Eu (444, 778, 1086, and 1408 keV), ^{133}Ba (356 keV), ^{137}Cs (662 keV), ^{60}Co (1173 and 1333), and. After calculating the linear attenuation coefficient (G_{LAC}) by first measuring the intensities of the gamma rays that were incident (I_o) and transmitted (I), the final value was used to calculate the mass attenuation coefficient (G_{MAC}). To get the values of the G_{LAC}, one must first calculate the slope of the linear graph that plots $Ln(I/I_o)$ against the sample thickness. Fig. 2 depicts the relationship between $Ln(I/I_o)$ and the sample thickness for all glasses measured at 662 keV. The patterns are nearly identical for all photon energies. As can be seen in Fig. 2, the average slope of the graph increases when

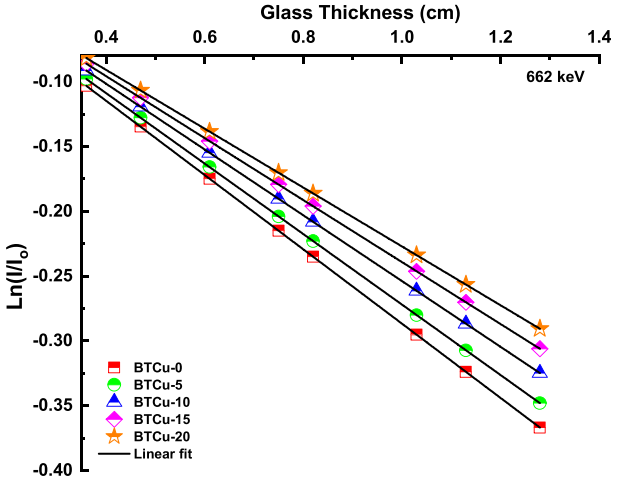

Fig. 2 – $Ln(I/I_o)$ against glass thickness for all glasses at 662 keV.

more TeO_2 and B_2O_3 are added to the mixture. The slope of the graph becomes more from 0.632 to 0.797 cm^{-1} at 238 keV, from 0.422 to 0.533 cm^{-1} at 356 keV, from 0.339 to 0.428 cm^{-1} at 444 keV, from 0.227 to 0.287 cm^{-1} at 662 keV, from 0.193 to 0.244 at 778 keV, from 0.165 to 0.208 cm^{-1} at 911, from 0.138 to 0.175 cm^{-1} at 1086 keV, from 0.128 to 0.162 cm^{-1} at 1173 keV, from 0.113 to 0.142 cm^{-1} at 1332 keV, and from 0.107 to 0.135 cm^{-1} at 1408 keV for BTCu-20, BTCu-15, BTCu-10, BTCu-5, and BTCu-0 samples, respectively. In this specific set of glasses, the glass with the highest TeO_2 content (BTCu-0) had the biggest gradient, which may be interpreted as having the highest GLAC values compared to the other glasses in the set. Consider that the Z of Te is 52, which is a value much more than the number for Cu (20). If a significant atomic number of Te is introduced to the structure of the glass, the interaction between gamma-ray photons and the atoms of Te will become more powerful. A larger quantity of photon energy must be absorbed before an electron can be released from a Te atom. This is because the higher the atomic number, the more complex the atom is. It's possible that the electron was ejected due to either the photoelectric effect or the Compton scattering, but it was not both. The quantity of gamma rays that are able to pass through the glass is less whenever there is a larger degree of interaction between the gamma rays and the target atom (Te). This directly contributed to the increase in the G_{LAC} that occurred [35]. The increase in the value of the G_{LAC} was also aided by the fact that the glass modifier was increased. This was still another factor. Incorporating a high modifier into the glass system (TeO_2 with a density of 6.04 g m^{-3}) is thought to be one way to reduce the porosity of the glass while simultaneously producing high glass. This theory is based on the fact that high modifiers tend to have larger surface areas than low modifiers. Glass will have a stronger attenuation than other materials since it has a lower porosity than other materials, which means there is a greater likelihood that gamma rays will interact with the atoms in glass [36].

Fig. 3 depicts the relationship between $Ln(I/I_o)$ and the sample thickness for BTCu-0 glass measured at 238, 356, 444, 662, 778, 911, 1086, 1173, 1332, and 1408 keV. The patterns are

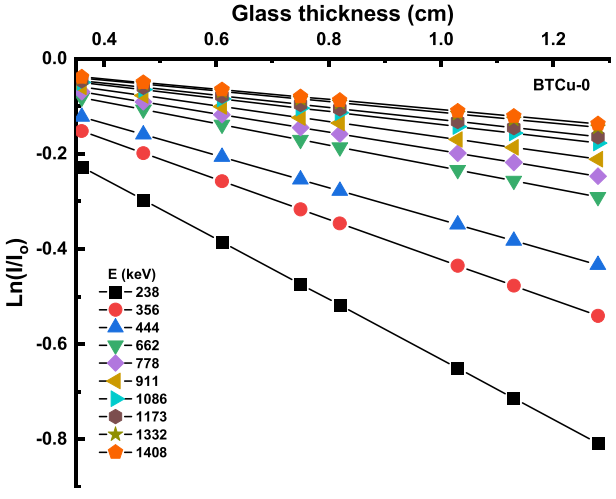

Fig. 3 – Ln(I/I_0) against glass thickness for BTCu-0 glass sample at studied photon energy.

nearly identical for BTCu-20, BTCu-15, BTCu-10, BTCu-5, and BTCu-0 glasses. As can be seen in Fig. 3, the average slope of the graph decreases when the photon energy increases from 238 to 1408 keV (Table 2). This indicates that when the energy is increased, the G_{LAC} values for particular glasses will fall. According to the findings, the G_{LAC} values reached their maximum at 238 keV and their minimum at 1408 keV.

G_{LAC} values for samples of BTCu-20, BTCu-15, BTCu-10, BTCu-5, and BTCu-0 are shown in Fig. 4 at energies of 238, 356, 444, 662, 778, 911, 1086, 1173, 1332, and 1408 keV respectively. If you look at the graph in Fig. 4, you'll observe that the G_{LAC} values grow higher when the concentration of TeO_2 gets increasing. This is a fact that may be seen for oneself. The BTCu-0 glass system has the highest G_{LAC} values of any other glass system. As was to be expected, the maximum G_{LAC} was brought about by the presence of TeO_2 in the glass system at its highest possible concentration. The higher the G_{LAC} values, the more effective a given material is in reducing the number of photons exposed. At the energies that were explored, it was discovered that increasing the quantity of TeO_2 in the glass samples led to an increase in the G_{LAC}. This was the result of what was discovered in the energies that were researched. The reason for this is that the presence of TeO_2 enhances both the effective atomic numbers of the elements and the density of the elements. As compared to other glasses, BTCu-0 glass, which had a TeO_2 content of 70 wt percent, had the maximum density, and hence, it had the highest G_{LAC} value. Research demonstrated that the BTCu-0 glass has the highest possible amount of photon interaction at the provided energy level. This interaction could take occur as a consequence of the photoelectric effect (PE), the Compton scattering (CS), or the production of pairs (PP). Irradiation of glass material by gamma-ray photons may generally be broken down into four distinct categories, depending on the specific circumstances: Photons interact with the glass through CS and pass through the glass. Atoms interact with photons through CS multiple times before being absorbed by PE [37]. (a) Photons pass through the glass without causing any interaction. (b) Photons are absorbed directly into the atoms that make up the structure of the glass through PE. (c) Photons interact with the glass through CS and pass through the glass. (d) Atoms interact with photons through CS for multiple. Fig. 5 presents the relative differences between the mass attenuation coefficient (GMAC) obtained using FLUKA simulation and that obtained by XCOM [38]. This figure shows that the Δ values are between 6 and -6%.

In addition, the effectiveness of gamma shielding may be discussed in terms of the half-value layer (G_{HVL}) and the mean free path (G_{MFP}). A material with a lower value of both the G_{HVL} and G_{MFP} might be used to generate a better shielding material. This could be the case. The average distance travelled by a photon between two successive contacts is referred to as the G_{MFP}. The G_{HVL} refers to the thickness of the material that is necessary to absorb fifty percent of the incoming radiation, and the G_{MFP} is the average distance that the photon must travel. The values of the G_{HVL} and G_{MFP} are shown in a scatter plot in each of Figs. 6 and 7, respectively. These plots are provided in the figures. There is a perceptible shift in both the G_{HVL} and G_{MFP} values of glasses after TeO_2 has been added. This change may be seen. Both the G_{HVL} and G_{MFP} values

Table 2 – The average slope of studied glasses at selected photon energy in keV.

Sample code	238	356	444	662	778	911	1086	1173	1332	1408
BTCu-0	0.797	0.533	0.428	0.287	0.244	0.208	0.175	0.162	0.142	0.135
BTCu-5	0.756	0.506	0.406	0.272	0.231	0.198	0.166	0.153	0.135	0.128
BTCu-10	0.706	0.472	0.379	0.254	0.216	0.184	0.155	0.143	0.126	0.119
BTCu-15	0.665	0.445	0.357	0.239	0.203	0.174	0.146	0.135	0.119	0.112
BTCu-20	0.632	0.422	0.339	0.227	0.193	0.165	0.138	0.128	0.113	0.107

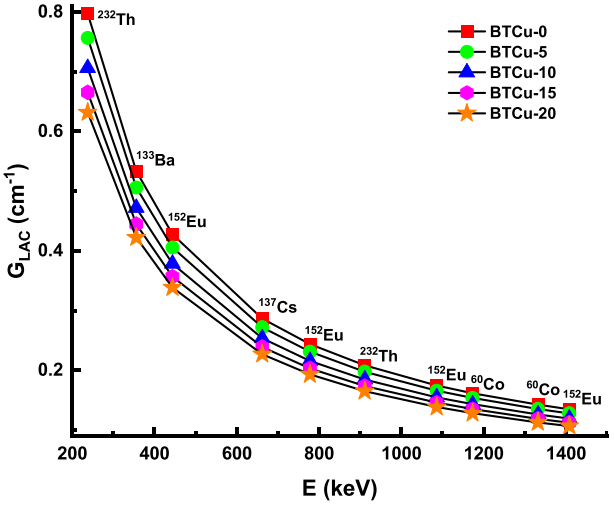

Fig. 4 – Linear attenuation coefficient (G_{LAC}) against photon energy for glass samples.

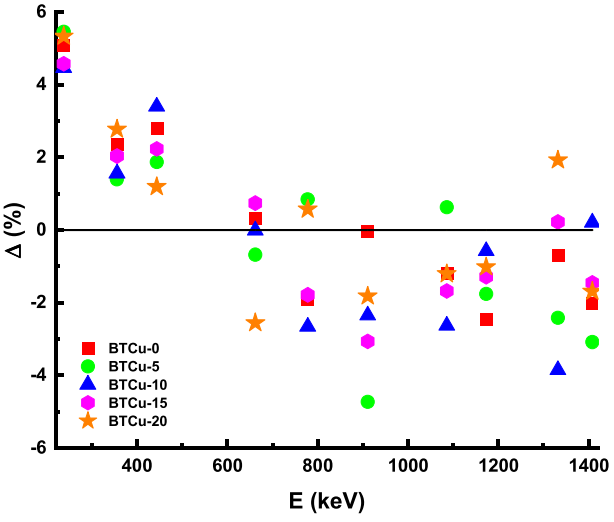

Fig. 5 – The relative difference (Δ, %) between G_{MAC} results the obtained using FLUKA code and that obtained via XCOM.

dropped as the mole percentage of TeO_2 reached its maximum amount. This was the case for both values. The growing trend of G_{HVL} and G_{MFP} values for glasses may be attributed to the increase in the density of glasses. This is because the density of glasses increases as their volume increases. The values of each parameter are seen to be dropping in this manner. According to the current research findings, the GHVL and GMFP

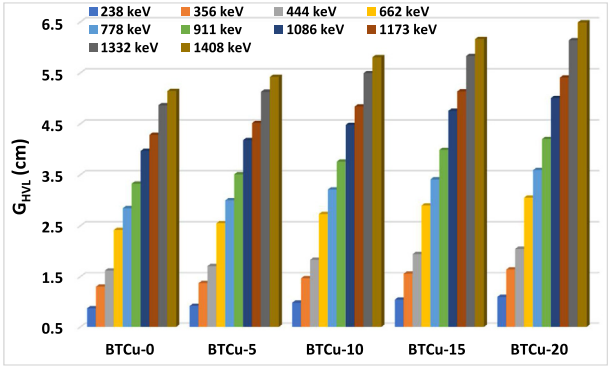

Fig. 6 – Half value layer (G_{HVL}) against glass composition at studied photon energy.

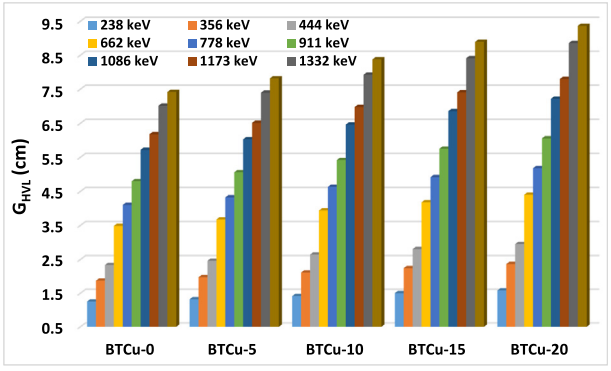

Fig. 7 – Mean free path (G_{MFP}) against glass composition at studied photon energy.

values of BTCu-0 glass come in at the bottom of the pack compared to those of other glasses. The G_{HVL} values for the BTCu-0 sample are as follows: 0.87, 1.30, 1.62, 2.42, 2.84, 3.33, 3.97, 4.28, 4.86, and 5.14 cm, respectively, when measured at 238, 356, 444, 662, 778, 911, 1086, 1173, 1332, and 1408 keV, respectively. The G_{MFP} values for the BTCu-0 sample are as follows: 1.25, 1.88, 2.34, 3.49, 4.10, 4.80, 5.72, 6.18, 7.02, and 7.42 cm when the sample is irradiated with 238, 356, 444, 662, 778, 911, 1086, 1173, 1332, and 1408 keV, respectively. This reveals that BTCu-0 glass is better than other forms of shielding glass in terms of its capability to minimize the number of photons generated by gamma rays and its overall efficacy. In view of the fact that the BTCu-0 has the lowest G_{HVL} value of the glasses that were tested, it is compared with a number of commonly used gamma shielding glasses, concretes, and polymers, as shown in Fig. 8(a–c) at 356, 662, 1173, and 1333 keV. The G_{HVL} value of the BTCu-0 glass has been

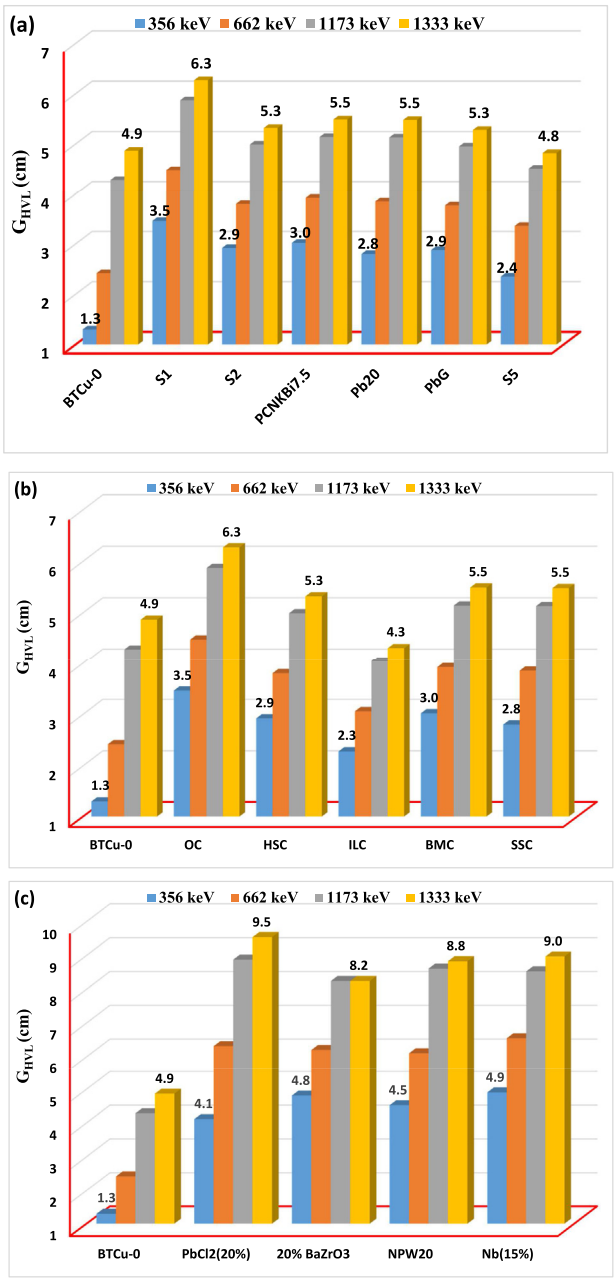

Fig. 8 – Half value layer values of BTCu-0 glass sample comparing to (a) glass materials, (b) some concrete, and (c) polymers at 356, 662, 1173, and 1333 keV.

shown to have a lower value than the G_{HVL} values of the various kinds of glass materials, concretes, and polymers that are shown in this figure. It indicates that this particular glass sample has a higher capacity for absorption than S1 [39], S2 [40], PCNKBi7.5 [41], Pb20 [42], PbG [43], S5 [44], (OC, HSC, ILC, BMC, IC) concretes [45], and PbCl2(20%) [46], 20% BaZrO3 [47], NPW20 [48], and Nb(15%) [49]. It has been shown that the glass that was generated as a result of the ongoing study is more effective than other glasses, concretes, and polymers when subjected to a certain photon energy. When these data are considered, it is feasible to conclude that BTCu-0 might be an alternative worth considering for use as a radiation shielding material.

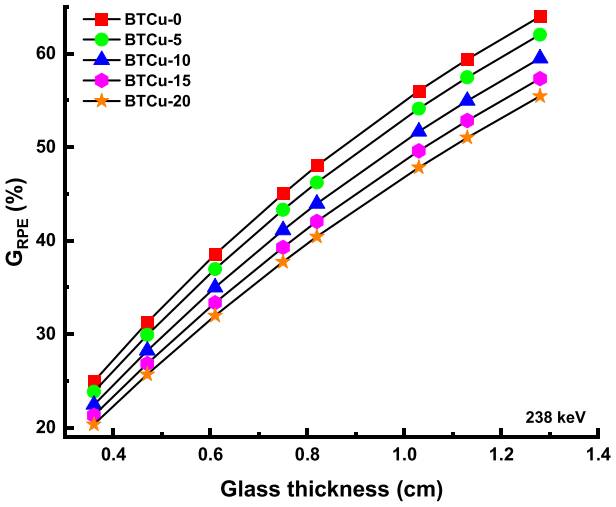

Fig. 9 – Radiation protection efficiency (G_{RPE}) against glass thickness for all glasses at 238 keV.

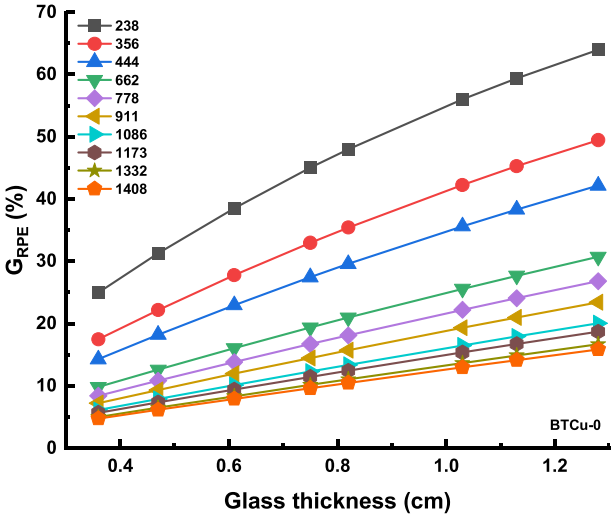

Fig. 10 – Radiation protection efficiency (G_{RPE}) for BTCu-0 glass sample at studied photon energy.

The gamma radiation protection efficiency, also known as G_{RPE}, is another key indicator that shows how effectively the glass absorbs photons. The GRPE values for the BTCu-20, BTCu-15, BTCu-10, BTCu-5, and BTCu-0 samples are shown in Fig. 9 for the following energies: 238, 356, 444, 662, 778, 911, 1086, 1173, 1332, and 1408 keV. As can be observed in this figure, the G_{RPE} values for glasses go up as the glass layer thickness and concentration go up, but they go down when the photon energy goes up (Fig. 10).

Based on our study of TeO_2–B_2O_3–CuO glass systems, we found that these materials demonstrate promising properties for radiation shielding, with variations in their efficiency depending on the concentration of CuO. These findings have significant practical implications. For example, glass systems could be used to construct safe storage for radioactive waste, where it is vital to shield the surrounding environment from emitted radiation. Similarly, they could be integrated into radiation therapy facilities, where protecting patients and

healthcare professionals from exposure to unnecessary radiation is essential. Furthermore, these glass systems could be used in space exploration. Spacecraft are exposed to high levels of cosmic radiation, and using these glass systems in spacecraft construction could provide the necessary protection for the onboard electronics and astronauts. We also recommend further research into the possibility of doping these glass systems with other elements or nanoparticles, as it might enhance their shielding efficiency. Our research opens new avenues for developing efficient, cost-effective, and environmentally friendly radiation shielding materials. However, more studies are needed to optimize their properties for specific applications.

4. Conclusion

In the present experiment, a glass modifier known as TeO_2 was used in order to increase the density of the glass system. This resulted in a denser system. It was found that the glasses with the highest concentration of TeO_2 generated the highest G_{LAC} while concurrently having the lowest G_{HVL} when compared to other kinds of glass. This was determined when several varieties of glass were compared to one another. Using gamma rays coming from various sources, the GLAC was calculated for each kind of glass at various photon energies. Because of the interaction between gamma-ray photons and the atoms of Te as well as the density of the glass modifier, the G_{LAC} values rose as the concentration of TeO_2 in the glass grew. This was ascribed to the fact that the glass modifier had a higher density. In addition, when the amount of energy increased, the G_{LAC} values for a particular kind of glass fell. This sample of glass provided a result that is even better than conventional concretes and some radiation-shielding polymers. This is because it is more resistant to radiation. This leads one to believe that this glass is superior to others in terms of its capacity to mitigate the harmful effects of gamma rays and the degree of protection it provides.

Declaration of competing interest

The authors declare that they have no known competing financial interests or personal relationships that could have appeared to influence the work reported in this paper.

Acknowledgments

This work was funded by the Dean of Scientific Research at Jouf University under Grant Number (DSR2022-RG-0127).

REFERENCES

[1] Aygün B. High alloyed new stainless steel shielding material for gamma and fast neutron radiation. Nucl Eng Technol 2020;52:647–53. https://doi.org/10.1016/j.net.2019.08.017.

[2] Alsaif NAM, Alotiby M, Hanfi MY, Sayyed MI, Mahmoud KA, Alotaibi BM, et al. A comprehensive study on the optical, mechanical, and radiation shielding properties of the TeO2–Li2O–GeO2 glass system. J Mater Sci Mater Electron 2021;32:15226–41. https://doi.org/10.1007/s10854-021-06074-3.

[3] Aygün B. Neutron and gamma radiation shielding Ni based new type super alloys development and production by Monte Carlo Simulation technique. Radiat Phys Chem 2021;188:109630. https://doi.org/10.1016/j.radphyschem.2021.109630.

[4] Kaewjaeng S, Kothan S, Chaiphaksa W, Chanthima N, Rajaramakrishna R, Kim HJ, et al. High transparency La2O3-CaO-B2O3-SiO2 glass for diagnosis x-rays shielding material application. Radiat Phys Chem 2019;160:41–7. https://doi.org/10.1016/j.radphyschem.2019.03.018.

[5] Şensoy AT, Gökçe HS. Simulation and optimization of gamma-ray linear attenuation coefficients of barite concrete shields. Construct Build Mater 2020;253:119218. https://doi.org/10.1016/j.conbuildmat.2020.119218.

[6] Tishkevich DI, Grabchikov SS, Lastovskii SB, Trukhanov SV, Zubar TI, Vasin DS, et al. Effect of the synthesis conditions and microstructure for highly effective electron shields production based on Bi coatings. ACS Appl Energy Mater 2018;1:1695–702. https://doi.org/10.1021/acsaem.8b00179.

[7] Tishkevich DI, Grabchikov SS, Lastovskii SB, Trukhanov SV, Vasin DS, Zubar TI, et al. Function composites materials for shielding applications: correlation between phase separation and attenuation properties. J Alloys Compd 2019;771:238–45. https://doi.org/10.1016/j.jallcom.2018.08.209.

[8] Alabsy MT, Alzahrani JS, Sayyed MI, Abbas MI, Tishkevich DI, El-Khatib AM, et al. Gamma-ray attenuation and exposure buildup factor of novel polymers in shielding using Geant4 simulation. Materials 2021;14:5051. https://doi.org/10.3390/ma14175051.

[9] Tishkevich DI, Zubar TI, Zhaludkevich AL, Razanau IU, Vershinina TN, Bondaruk AA, et al. Isostatic hot pressed W–Cu composites with nanosized grain boundaries: microstructure, structure and radiation shielding efficiency against gamma rays. Nanomaterials 2022;12:1642. https://doi.org/10.3390/nano12101642.

[10] Dong M, Zhou S, Xue X, Feng X, Yang H, Sayyed MI, et al. Upcycling of boron bearing blast furnace slag as highly cost-effective shield for protection of neutron radiation hazard: an innovative way and proposal of shielding mechanism. J Clean Prod 2022;355:131817. https://doi.org/10.1016/j.jclepro.2022.131817.

[11] Aloraini DA, Almuqrin AH, Sayyed MI, Kumar A, Gaikwad DK, Tishkevich DI, et al. Experimental and theoretical analysis of radiation shielding properties of strontium-borate-tellurite glasses. Opt Mater 2021;121:111589. https://doi.org/10.1016/j.optmat.2021.111589.

[12] Tishkevich DI, Grabchikov SS, Grabchikova EA, Vasin DS, Lastovskiy SB, Yakushevich AS, et al. Modeling of paths and energy losses of high-energy ions in single-layered and multilayered materials. IOP Conf Ser Mater Sci Eng 2020;848:012089. https://doi.org/10.1088/1757–899X/848/1/012089.

[13] Issa SAM, Sayyed MI, Zaid MHM, Matori KA. Photon parameters for gamma-rays sensing properties of some oxide of lanthanides. Results Phys 2018;9:206–10. https://doi.org/10.1016/j.rinp.2018.02.039.

[14] Oto B, Kavaz E, Durak H, Aras A, Madak Z. Effect of addition of molybdenum on photon and fast neutron radiation shielding properties in ceramics. Ceram Int 2019;45:23681–9. https://doi.org/10.1016/j.ceramint.2019.08.082.

[15] Abouhaswa AS, Kavaz E. A novel B2O3-Na2O-BaO-HgO glass system: synthesis, physical, optical and nuclear shielding features. Ceram Int 2020;46:16166–77. https://doi.org/10.1016/j.ceramint.2020.03.172.
[16] Chanthima N, Kaewkhao J, Limkitjaroenporn P, Tuscharoen S, Kothan S, Tungjai M, et al. Development of BaO–ZnO–B2O3 glasses as a radiation shielding material. Radiat Phys Chem 2017;137:72–7. https://doi.org/10.1016/j.radphyschem.2016.03.015.
[17] Mustafa I, Kamari H, Yusoff W, Aziz S, Rahman A. Structural and optical properties of lead-boro-tellurrite glasses induced by gamma-ray. Int J Mol Sci 2013;14:3201–14. https://doi.org/10.3390/ijms14023201.
[18] Azlina Y, Azlan MN, Halimah MK, Umar SA, El-Mallawany R, Najmi G. Optical performance of neodymium nanoparticles doped tellurite glasses. Phys B Condens Matter 2020;577:411784. https://doi.org/10.1016/j.physb.2019.411784.
[19] Tafida RA, Halimah MK, Muhammad FD, Chan KT, Onimisi MY, Usman A, et al. Structural, optical and elastic properties of silver oxide incorporated zinc tellurite glass system doped with Sm3+ ions. Mater Chem Phys 2020;246:122801. https://doi.org/10.1016/j.matchemphys.2020.122801.
[20] Aktas B, Acikgoz A, Yilmaz D, Yalcin S, Dogru K, Yorulmaz N. The role of TeO2 insertion on the radiation shielding, structural and physical properties of borosilicate glasses. J Nucl Mater 2022;563:153619. https://doi.org/10.1016/j.jnucmat.2022.153619.
[21] Fidan M, Acikgoz A, Demircan G, Yilmaz D, Aktas B. Optical, structural, physical, and nuclear shielding properties, and albedo parameters of TeO2–BaO–B2O3–PbO–V2O5 glasses. J Phys Chem Solid 2022;163:110543. https://doi.org/10.1016/j.jpcs.2021.110543.
[22] Çetın B, Yalçin Ş, Aktas B, Albaşkara M. Investigation of radiation shielding properties of soda-lime-silica glasses doped with different food materials. Acta Phys Pol, A 2017;132:988–90. https://doi.org/10.12693/APhysPolA.132.988.
[23] Umar SA, Halimah MK, Chan KT, Latif AA. Physical, structural and optical properties of erbium doped rice husk silicate borotellurite (Er-doped RHSBT) glasses. J Non-Cryst Solids 2017;472:31–8. https://doi.org/10.1016/j.jnoncrysol.2017.07.013.
[24] Azlina Y, Azlan MN, Hajer SS, Halimah MK, Suriani AB, Umar SA, et al. Graphene oxide deposition on neodymium doped zinc borotellurite glass surface: optical and polarizability study for future fiber optics. Opt Mater 2021;117:111138. https://doi.org/10.1016/j.optmat.2021.111138.
[25] El-Moneim AA, Eltohamy M, Afifi H, Gaafar MS, Atef A. An ultrasonic study on ternary xPbO–(45-x)CuO–55B2O3 glasses. Ceram Int 2021;47:27351–60. https://doi.org/10.1016/j.ceramint.2021.06.157.
[26] Attallah M, Farouk M, El-Korashy A, ElOkr M. Copper doped phosphate glass as an optical bandpass filter. Silicon 2018;10:547–54. https://doi.org/10.1007/s12633-016-9488-7.
[27] Umar SA, S.N N, Geidam IG, El-Mallawany R, Abd-Elnaiem A M, Hakamy A, et al. Optical basicity, polarizability and spectroscopic investigations of CuO doped TeO2–B2O3 glass system. Mater Chem Phys 2023;297:127309. https://doi.org/10.1016/j.matchemphys.2023.127309.
[28] Sharma A, Nazrin SN, Humaira SA, Boukhris I, Kebaili I. Impact of neodymium oxide on optical properties and X-ray shielding competence of Nd2O3–TeO2–ZnO glasses. Radiat Phys Chem 2022;195:110047. https://doi.org/10.1016/j.radphyschem.2022.110047.
[29] Battistoni G, Boehlen T, Cerutti F, Chin PW, Esposito LS, Fassò A, et al. Overview of the FLUKA code. Ann Nucl Energy 2015;82:10–8. https://doi.org/10.1016/j.anucene.2014.11.007.
[30] Madbouly AM, Sallam OI, Issa SAM, Rashad M, Hamdy A, Tekin HO, et al. Experimental and FLUKA evaluation on structure and optical properties and γ-radiation shielding capacity of bismuth borophosphate glasses. Prog Nucl Energy 2022;148:104219. https://doi.org/10.1016/j.pnucene.2022.104219.
[31] Tekin HO, Kassab LRP, Issa SAM, Dias da Silva Bordon C, Al-Buriahi MS, de Oliviera Pereira Delboni F, et al. Structural and physical characterization study on synthesized tellurite (TeO_2) and germanate (GeO_2) glass shields using XRD, Raman spectroscopy, FLUKA and PHITS. Opt Mater 2020;110. https://doi.org/10.1016/j.optmat.2020.110533.
[32] Mostafa AMA, Zakaly HMH, Pyshkina M, Issa SAM, Tekin HO, Sidek HAA, et al. Multi-objective optimization strategies for radiation shielding performance of BZBB glasses using Bi2O3: a FLUKA Monte Carlo code calculations. J Mater Res Technol 2020;9:12335–45. https://doi.org/10.1016/j.jmrt.2020.08.077.
[33] Ferrari a, Sala PR, Fasso A, Ranft J. FLUKA: A Multi-Particle Transport Code. CERN-2005-10 2005:INFN/TC 05/11, SLAC-R-773. https://doi.org/10.2172/877507.
[34] Alatawi A, Alsharari AM, Issa SAM, Rashad M, Darwish AAA, Saddeek YB, et al. Improvement of mechanical properties and radiation shielding performance of AlBiBO3 glasses using yttria: an experimental investigation. Ceram Int 2020;46:3534–42. https://doi.org/10.1016/j.ceramint.2019.10.069.
[35] Issa SAM, Mostafa AMA. Effect of Bi2O3in borate-tellurite-silicate glass system for development of gamma-rays shielding materials. J Alloys Compd 2017;695:302–10. https://doi.org/10.1016/j.jallcom.2016.10.207.
[36] Bagheri R, Khorrami Moghaddam A, Yousefnia H. Gamma ray shielding study of barium–bismuth–borosilicate glasses as transparent shielding materials using MCNP-4C code, XCOM program, and available experimental data. Nucl Eng Technol 2017;49:216–23. https://doi.org/10.1016/j.net.2016.08.013.
[37] Çelikbilek Ersundu M, Ersundu AE, Sayyed MI, Lakshminarayana G, Aydin S. Evaluation of physical, structural properties and shielding parameters for K 2 O–WO 3 –TeO 2 glasses for gamma ray shielding applications. J Alloys Compd 2017;714:278–86. https://doi.org/10.1016/j.jallcom.2017.04.223.
[38] Berger MJ, Hubbell JH. XCOM: Photon cross sections on a personal computer. Oak Ridge, TN. 1987. https://doi.org/10.2172/6016002.
[39] Aktas B, Yalcin S, Dogru K, Uzunoglu Z, Yilmaz D. Structural and radiation shielding properties of chromium oxide doped borosilicate glass. Radiat Phys Chem 2019;156:144–9. https://doi.org/10.1016/j.radphyschem.2018.11.012.
[40] Yalcin S, Aktas B, Yilmaz D. Radiation shielding properties of Cerium oxide and Erbium oxide doped obsidian glass. Radiat Phys Chem 2019;160:83–8. https://doi.org/10.1016/j.radphyschem.2019.03.024.
[41] Mhareb MHA, Alajerami YSM, Sayyed MI, Dwaikat N, Alqahtani M, Alshahri F, et al. Radiation shielding, structural, physical, and optical properties for a series of borosilicate glass. J Non-Cryst Solids 2020;550:120360. https://doi.org/10.1016/j.jnoncrysol.2020.120360.
[42] Al-Yousef HA, Sayyed MI, Alotiby M, Kumar A, Alghamdi YS, Alotaibi BM, et al. Evaluation of optical, and radiation shielding features of New phosphate-based glass system. Optik 2021;242:167220. https://doi.org/10.1016/j.ijleo.2021.167220.
[43] Al-Harbi FF, Prabhu NS, Sayyed MI, Almuqrin AH, Kumar A, Kamath SD. Evaluation of structural and gamma ray shielding competence of Li2O-K2O-B2O3-HMO (HMO = SrO/TeO2/PbO/Bi2O3) glass system. Optik 2021;248:168074. https://doi.org/10.1016/j.ijleo.2021.168074.

[44] Singh S, Kaur R, Rani S, Sidhu BS. Physical, structural and nuclear radiation shielding behaviour of xBaO-(0.30-x)MgO-0.10Na2O-0.10Al2O3-0.50B2O3 glass matrix. Mater Chem Phys 2022;276:125415. https://doi.org/10.1016/j.matchemphys.2021.125415.

[45] Bashter II. Calculation of radiation attenuation coefficients for shielding concretes. Ann Nucl Energy 1997;24:1389–401. https://doi.org/10.1016/S0306-4549(97)00003-0.

[46] Özkalaycı F, Kaçal MR, Agar O, Polat H, Sharma A, Akman F. Lead(II) chloride effects on nuclear shielding capabilities of polymer composites. J Phys Chem Solid 2020;145:109543. https://doi.org/10.1016/j.jpcs.2020.109543.

[47] Ozel F, Akman F, Kaçal MR, Ozen A, Arslan H, Polat H, et al. Production of microstructured BaZrO3 and Ba2P2O7-based polymer shields for protection against ionizing photons. J Phys Chem Solid 2021;158:110238. https://doi.org/10.1016/j.jpcs.2021.110238.

[48] Tekin HO, Kaçal MR, Issa SAM, Polat H, Susoy G, Akman F, et al. Sodium dodecatungstophosphate hydrate-filled polymer composites for nuclear radiation shielding. Mater Chem Phys 2020;256:123667. https://doi.org/10.1016/j.matchemphys.2020.123667.

[49] Akman F, Ogul H, Ozkan I, Kaçal MR, Agar O, Polat H, et al. Study on gamma radiation attenuation and non-ionizing shielding effectiveness of niobium-reinforced novel polymer composite. Nucl Eng Technol 2021. https://doi.org/10.1016/j.net.2021.07.006.